

Forward Production With Large p/π Ratio and Without Jet Structure at Any p_T

Rudolph C. Hwa¹ and C. B. Yang²

¹Institute of Theoretical Science and Department of Physics
University of Oregon, Eugene, OR 97403-5203, USA

²Institute of Particle Physics, Hua-Zhong Normal University, Wuhan 430079, P. R. China

Abstract

Particle production in the forward region of heavy-ion collisions is shown to be due to parton recombination without shower partons. The regeneration of soft partons due to momentum degradation through the nuclear medium is considered. The degree of degradation is determined by fitting the \bar{p}/p ratio. The data at $\sqrt{s} = 62.4$ GeV and $\eta = 3.2$ from BRAHMS on the p_T distribution of average charged particles are well reproduced. Large proton-to-pion ratio is predicted. The particles produced at any p_T should have no associated particles above background to manifest any jet structure.

PACS numbers: 25.75.Dw

1 Introduction

In an earlier paper [1] we studied the problem of hadron production in the transfragmentation region (TFR) in heavy-ion collisions. It was stimulated by the data of PHOBOS [2] that show the detection of charged particles at $\eta' > 0$, where $\eta' = \eta - y_{\text{beam}}$. We broadly refer to the $\eta' > 0$ region as TFR. However, since the transverse momenta p_T of the particles were not measured, it has not been possible to determine the corresponding values of Feynman x , in terms of which TFR can more precisely be defined as the region with $x > 1$. More recently, BRAHAMS has analyzed their forward production data at $\sqrt{s} = 62.4$ GeV with both η and p_T determined [3]. It is then possible to interpret BRAHAMS data by applying the formalism developed in [1], which is done entirely in the framework of using momentum fractions instead of η . In this paper we calculate the proton and pion distributions in x and p_T and conclude not only that the p/π ratio is large, but also that there should be no jet structure associated with the particles detected at any p_T in the forward region.

In [1] the x distributions of p and π have been calculated for $0.6 < x < 1.2$ in the recombination model [4, 5, 6], taking into account momentum degradation of particle constituents traversing nuclear matter [7] and the recombination of partons arising from different beam nucleons. However, we have not considered the regeneration of soft partons as a consequence of momentum degradation in the nuclear medium. Since such soft partons significantly increase the antiquark distribution in the mid- x region, it is important to include them in the determination of the pion distribution. Furthermore, no consideration has been given in [1] to transverse momentum, which is the other major concern in this paper.

In the following we use forward production to refer specifically to hadrons produced at $x > 0.3$, with the fragmentation region (FR) being $0.3 < x < 1$, and TFR being $x > 1$. Any hadron produced in the TFR cannot be due to the fragmentation of any parton because of momentum conservation, since no parton can have momentum fraction > 1 , if we ignore the minor effect of Fermi motion of the nucleons in a nucleus. In the FR hadrons with any p_T that are kinematically allowed can, in principle, arise from the fragmentation of hard partons; however, the momenta of those hard partons must be even higher than the detected hadrons in the FR, and the probability of hard scattering into the region near the kinematical boundary is severely suppressed [8]. Moreover, there is the additional suppression due to the fragmentation function from parton to hadron. Thus the fragmentation of partons at any p_T in the FR (despite the nomenclature that has its roots in reference to the fragmentation of the incident hadron) is highly unlikely, though not impossible. The issue to focus on is then to examine whether there can be any hadrons produced in the FR with any significant p_T . If so, then such hadrons at any p_T would not be due to fragmentation and would therefore not have any associated jet structure.

In contrast to the double suppression discussed above in connection with fragmentation, recombination benefits from double support from two factors. One is the additivity of the parton momenta in hadronization, thus allowing the contributing partons to be at lower x where the density of partons is higher. The other is that those partons can arise from different forward-going nucleons, thus making possible the sum of their momentum fractions to vary smoothly across $x = 1$, thereby amalgamating FR with TFR. These are the two attributes of the recombination process that makes it particularly relevant for forward production. Its implementation, however, relies on two extensions of what has been considered in [1], namely, the regeneration of soft partons and the transverse-momentum aspect of the problem, before we can compare our results with BRAHMS data [3].

It is useful to outline the logical connections among the different parts of this work. First of all, the degree of degradation of forward momenta through the nuclear medium is unknown. The degradation parameter κ can be determined phenomenologically if the x distributions of the forward proton and pion are known, but they are not. We have calculated the x distributions for $\kappa = 0.6$ and 0.8 as typical values serving as benchmarks. Since the normalization of the p_T distribution, which is known from BRAHMS data [3], depends on the x distribution, κ can be determined by fitting the p_T distribution. However, what is known about the p_T distribution is only for all charged particles, not p or π separately. If there were experimental data on the p/π ratio (which is not yet available for the 62.4 GeV data that have the p_T distribution), one could disentangle the species dependence. Fortunately, there exist preliminary data on \bar{p}/p and K/π ratios at 62.4 GeV. We shall therefore calculate the p and \bar{p} distributions and adjust κ to render the ratio $R_{\bar{p}/p}$ to be in the vicinity of the observed ratio. We shall then show that the p_T distribution of all charged particles can be well reproduced in our calculation.

We shall assume factorizability in p_L and p_T dependences. The two are treated in Sec. II and III, respectively. The main difference between Sec. II and the earlier work in [1] is the inclusion of the regeneration of soft partons, a subject we now address.

2 Regeneration of Soft Partons

Let us first recall some basic equations from Ref. [1], which we shall refer to as I. Equations I-(16) and I-(32) give the proton and pion distributions in x (with the p_T variables integrated out) for AB collisions in the recombination model

$$H_p^{AB}(x) = \int \frac{dx_1}{x_1} \frac{dx_2}{x_2} \frac{dx_3}{x_3} F_{uud}^{AB}(x_1, x_2, x_3) R_p(x_1, x_2, x_3, x) , \quad (1)$$

$$H_\pi^{AB}(x) = \int \frac{dx_1}{x_1} \frac{dx_2}{x_2} F_{q\bar{q}}^{AB}(x_1, x_2) R_\pi(x_1, x_2, x) . \quad (2)$$

where the hadronic x is $2p_L/\sqrt{s}$ and the partonic x_i are momentum fractions. The recombination functions R_p and R_π are given in [1]. The partons are assumed to arise from different nucleons in the projectile nucleus A and thus contribute in factorizable form of F^{AB} , i.e.,

$$F_{uud}^{AB}(x_1, x_2, x_3) = F_{\bar{\nu}}^u(x_1) F_{\bar{\nu}}^u(x_2) F_{\bar{\nu}}^d(x_3) , \quad (3)$$

$$F_{q\bar{q}}^{AB}(x_1, x_2) = F_{\bar{\nu}}^q(x_1) F_{\bar{\nu}}^{\bar{q}}(x_2) , \quad (4)$$

where $\bar{\nu}$ is the average number of wounded nucleons that a nucleon encounters in traversing the nucleus B at a particular impact parameter, given in Eq. I-(49). The effect of momentum degradation on the parton distributions is contained in the expressions

$$F_{\bar{\nu}}^q(x_i) = \int_{x_i}^1 dy' \bar{G}'_{\bar{\nu}}(y') K\left(\frac{x_i}{y'}\right) , \quad (5)$$

$$F_{\bar{\nu}}^{\bar{q}}(x_i) = \int_{x_i}^1 dy' \bar{G}'_{\bar{\nu}}(y') L'_q\left(\frac{x_i}{y'}\right) , \quad (6)$$

$$\bar{G}'_{\bar{\nu}}(y') = \sum_{\nu=0}^{\infty} \kappa^{-2\nu} G(\kappa^{-\nu} y') \frac{\bar{\nu}^\nu}{\nu!} e^{-\bar{\nu}} , \quad (7)$$

where κ is the average momentum fraction of a valon after each collision and $G(y)$ is the valon distribution in momentum fraction y before collision [9]. $K(z)$ and $L'_q(z)$ are the quark distributions in a valon, with

$$K(z) = K_{NS}(z) + L'_q(z) , \quad (8)$$

$K_{NS}(z)$ being the valence-quark distribution and $L'_q(z)$ the saturated sea-quark distribution after gluon conversion. This briefly summarizes the essence of determining the x distributions of protons and pions produced in AB collisions.

To describe how the above should be modified in order to take into account the regeneration of soft partons, we need to fill in the steps on how sea-quark distribution $L'_q(z)$ is derived. In addition to the valence quark in a valon, there are also sea quarks (q), strange quark (s) and gluons (g), whose distributions are denoted by $L_i(z)$, $i = q, s, g$. Their second moments satisfy the sum rule for momentum conservation [1, 9]

$$\tilde{K}_{NS}(2) + 2 \left[2\tilde{L}_q(2) + \tilde{L}_s(2) \right] + \tilde{L}_g(2) = 1 . \quad (9)$$

Gluon conversion to $q\bar{q}$ changes the sea-quark distribution to

$$L'_{q,s}(z) = Z_1 L_{q,s}(z) , \quad (10)$$

whose second moment satisfies the modified version of Eq. (9) where $\tilde{L}_g(2)$ is absent, i.e.,

$$\tilde{K}_{NS}(2) + 2 \left[2\tilde{L}'_q(2) + \tilde{L}'_s(2) \right] = 1 . \quad (11)$$

From these equations we can determine Z_1 , getting

$$Z_1 = 1 + \frac{\tilde{L}_g(2)}{2 \left[2\tilde{L}_q(2) + \tilde{L}_s(2) \right]} . \quad (12)$$

This is what we obtained and used in I to calculate the hadron distributions.

The degradation effect is parametrized by κ such that $1 - \kappa$ is the fraction of momentum lost by a valon after a collision. After ν collisions, the net momentum fraction lost is $1 - \kappa^\nu$. That fraction is converted to soft partons so that the new sea-quark distributions $L''_{q,s}(z)$ satisfy a sum rule that differs from Eq. (11) by the addition of extra momentum available for conversion, i.e.,

$$\tilde{K}_{NS}(2) + 2 \left[2\tilde{L}''_q(2) + \tilde{L}''_s(2) \right] = 1 + (1 - \kappa^\nu) . \quad (13)$$

Assuming that only the normalization is changed, we write

$$L''_{q,s}(z, \kappa, \nu) = Z_2(\kappa, \nu) L_{q,s}(z) , \quad (14)$$

which yields, upon using Eqs. (9) and (13),

$$Z_2(\kappa, \nu) = 1 + \frac{1 - \kappa^\nu + \tilde{L}_g(2)}{2 \left[2\tilde{L}_q(2) + \tilde{L}_s(2) \right]} . \quad (15)$$

In [1] we have considered the cases: $\kappa = 0.6$ and 0.8 for $b = 1$ fm (0-5%) and 8 fm (30-40%). For any given b , the average $\bar{\nu}$ is known [see Eq. I-(12), (13)]. The dependence of ν on $\bar{\nu}$ is Poissonian, as expressed in the last factor in Eq. (7). We now replace $L'_q(z)$ in Eqs. (6) and (8) by $L''_q(z, \kappa, \nu)$ and obtain the new distributions $F_{\bar{\nu}}^q(x_i, \kappa)$ and $F_{\bar{\nu}}^{\bar{q}}(x_i, \kappa)$ defined in Eqs. (5) and (6), in which the summation over ν in $\bar{G}'_{\bar{\nu}}(y')$ is now extended to include the ν dependence of $L''_q(z, \kappa, \nu)$. As an illustration of our results on the effects of degradation and regeneration, we show in Fig. 1 the u -quark, $F_{\bar{\nu}}^u(x)$, and \bar{u} -antiquark, $F_{\bar{\nu}}^{\bar{u}}(x)$, distributions before and after regeneration for $b = 1$ mb and $\kappa = 0.6$. Note that with or without regeneration all distributions are highly peaked at $x = 0$ because momentum degradation pushes all valons to lower momenta by a factor of $\kappa^{\bar{\nu}}$ (which for $\bar{\nu} \sim 6$ is $\sim 1/20$). Regeneration increases $F_{\bar{\nu}}^{\bar{u}}(x)$ significantly for $x < 0.3$, as shown by the dashed-dotted line above the dotted line. For $F_{\bar{\nu}}^u(x)$, because of the dominance of the valence quark distribution $K_{NS}(z)$, the increase is minimal, as the dashed line is nearly all covered by the solid line. Similar changes occur for the d and \bar{d} distributions.

In the same way as we have done in [1] we calculate the proton and pion distributions in x for $\kappa = 0.6$ and 0.8 and for $b = 1$ and 8 fm. The results are shown in Figs. 2-5. Since

the regenerated soft partons do not affect the hadron distributions for $x > 0.8$ (remembering that the hadron x is the sum of the parton x_i), we have plotted these figures for the range $0.3 < x < 0.9$. We emphasize here that the large x behavior in the TFR is not the central issue in this paper any more, as it was in [1].

In Figs. 2-5, in addition to our present result with regeneration (solid and dashed lines) we show also our previous result obtained in [1] without regeneration for the case $\kappa = 0.6$ for the purpose of seeing the effect of regeneration. Note that the proton distributions in Figs. 2 and 3 are not affected very much by the regeneration effect, but the pion distributions in Figs. 4 and 5 are increased. At $x = 0.6$ the increase is roughly around a factor of 3.

In [1] there was no data to compare with the calculated result on the x distributions. In particular, the degree of momentum degradation was unknown. Now, BRAHMS data show the p_T dependence at $\eta = 3.2$ [3]. In order to fit the p_T distributions of the hadrons produced, we must have the correct normalizations, which in turn depend on the x distributions that we have studied.

3 Transverse Momentum Distribution

Having determined the longitudinal part of the hadronic distributions above, modulo the value of κ , we now proceed to the transverse part. We have treated the degradation and regeneration problems on rather general grounds without restricting the x values and with p_T integrated so that p_T never appears in our consideration of the x distribution. It is then natural to make use of that result in a factorizable form for the inclusive distribution

$$\frac{x}{p_T} \frac{dN_h}{dxdp_T} = H_h(x, \kappa) V_h(p_T), \quad (16)$$

which is, of course, an assumed form that is sensible when there is negligible contribution from hard scattering.

For the transverse part, $V_h(p_T)$, we follow the same type of consideration as developed in [6], where particle production at intermediate p_T is shown to be dominated by the recombination process. Similar work in that respect has also been done in [10, 11]. In the absence of hard scattering there are no shower partons. Without shower partons there are only thermal partons to recombine. Thus for pion production we have $\mathcal{T}\mathcal{T}$ recombination, while for proton we have $\mathcal{T}\mathcal{T}\mathcal{T}$ recombination, where \mathcal{T} represents the thermal parton distribution [6]

$$\mathcal{T}(p_{1T}) = p_{iT} \frac{dN^{\text{th}}}{dp_{iT}} = C_i p_{iT} \exp(-p_{iT}/T). \quad (17)$$

In the above equation p_{iT} is the transverse momentum of i th parton; C_i and T are two parameters as yet undetermined for the forward region in Au+Au collisions. In view of the factorization in Eq. (16) we use the term thermal in the sense of local thermal equilibrium of the partons in the co-moving frame of a fluid cell whose velocity in the cm system corresponds to the longitudinal momentum fraction x . However, the value of T can include radial flow effect.

Limiting ourselves to only the transverse component, the invariant distributions of produced pion and proton due to thermal-parton recombination are

$$\frac{dN_\pi^{\text{th}}}{p_T dp_T} \propto C_q C_{\bar{q}} \exp(-p_T/T), \quad (18)$$

$$\frac{dN_p^{\text{th}}}{p_T dp_T} \propto C_q^3 p_T \exp(-p_T/T), \quad (19)$$

where the proportionality factors that depend on the recombination functions are given in [6]. At midrapidity, thermal and chemical equilibrium led us to assume $C_q = C_{\bar{q}}$, and we have been able to obtain p/π ratio in good agreement with the data. Now, in FR (and in TFR) we must abandon chemical equilibrium, since \bar{q} cannot have the same density as q , when x is large. But we do retain thermal equilibrium within each species of partons to justify Eqs. (18) and (19) for the p_T dependence. We join the longitudinal and transverse parts of the problem by requiring

$$C_q \propto F_\nu^q(x_i, \kappa), \quad C_{\bar{q}} \propto F_{\bar{\nu}}^{\bar{q}}(x_j, \kappa), \quad (20)$$

where $F_\nu^q(x_i, \kappa)$ and $F_{\bar{\nu}}^{\bar{q}}(x_j, \kappa)$ are the quark and antiquark distributions in their respective momentum fractions already studied in Sec. II above. The proportionality factors in the two expressions above are the same. Equation (20) connects the parton density from the study of the longitudinal motion to the thermal distribution in the transverse motion. Substituting those relations into Eqs. (18) and (19), and letting $F_\nu^q(x_i, \kappa)$, $F_{\bar{\nu}}^{\bar{q}}(x_j, \kappa)$ and other multiplicative factors be absorbed in the formulas for $H_h(x, \kappa)$ developed in [1], we obtain for the transverse part of Eq. (16)

$$V_\pi(p_T) = c_\pi^2 \exp(-p_T/T), \quad (21)$$

$$V_p(p_T) = c_p^3 p_T \exp(-p_T/T), \quad (22)$$

where c_π and c_p are two proportionality constants to be determined by the normalization condition

$$\int_0^\infty dp_T p_T V_h(p_T) = 1, \quad (23)$$

i.e.,

$$c_\pi = 1/T, \quad c_p = 1/(2^{1/3}T). \quad (24)$$

It follows from Eqs. (16) and (23) that we recover the invariant x -distribution

$$x \frac{dN_h}{dx} = H_h(x, \kappa) \quad (25)$$

without undetermined proportionality factors.

The exponential factors in Eqs. (21) and (22) give the characteristic behavior of hadrons produced by the recombination of thermal partons [6, 8]. Such exponential behavior is overwhelmed by power-law behavior at intermediate p_T due to thermal-shower recombination when x is small and when light quarks contribute to the hadrons produced. However, when x is large, the shower partons are absent due to the suppression of hard scattering, so the exponential p_T dependence becomes the prevalent behavior in the forward region. Since the data of BRAHMS [3] exhibit the p_T distribution for a narrow range of η around 3.2, we can readily check whether Eqs. (16), (21) and (22) are in accord with the data. We consider only the most central collisions for which $H_\pi(x, \kappa)$ and $H_p(x, \kappa)$ have been calculated in the previous section for $b = 1$ fm. The data of the p_T distribution in [3] are, however, given for average charged particle $(h^+ + h^-)/2$. To be able to make comparison with that, we need information on the magnitudes of contributions from K and \bar{p} . Preliminary data on the K/π ratio is ~ 0.15 [12], and that on the \bar{p}/p ratio is ~ 0.05 [13]. We shall use the former ratio and calculate the latter.

The enhanced \bar{q} distribution enables us to compute $H_{\bar{p}}(x, \kappa)$ exactly as in Eq. (1), except that $F_\nu^q(x_j)$ in Eq. (3) is replaced by $F_\nu^{\bar{q}}(x_j)$. The \bar{p}/p ratio is constant in p_T , since both p and \bar{p} have the same p_T dependence given in Eq. (22). The value of the ratio, however, depends on $H_{\bar{p}}(x, \kappa)$ and $H_p(x, \kappa)$. The value of x for both p and \bar{p} is chosen to be 0.55 for reasons to be explained below when we discuss the p_T distribution. Since the data on \bar{p}/p are preliminary and imprecise at this point, we consider two values of κ and obtain

$$\begin{aligned} \kappa &= 0.76, & R_{\bar{p}/p} &= 0.031, \\ \kappa &= 0.72, & R_{\bar{p}/p} &= 0.058. \end{aligned} \quad (26)$$

These results bracket the observed value of \bar{p}/p at ~ 0.05 for $\sqrt{s} = 62.4$ GeV and $\eta = 3.2$ [13]. Note that with a 5% decrease in κ there is over 80% increase in \bar{p}/p . This is a direct consequence of soft-parton regeneration, where enhanced \bar{q} distribution significantly increases the \bar{p} production. To learn about the effect of regeneration, we have calculated $H_{\bar{p}}(x, \kappa)$ with the soft-parton regeneration turned off, and found that for $x_{\bar{p}} = 0.55$ and $\kappa = 0.76$ the ratio of the corresponding $H_{\bar{p}}(x, \kappa)$ values with regeneration to that without is about 2000. In other words without regeneration $R_{\bar{p}/p}$ would be at the level of 2.5×10^{-5} , which is hardly measurable.

The increase of \bar{p} production due to regeneration is much more than the corresponding increase of π (shown in Fig. 4) for a good reason. It is not just a matter of \bar{p} consisting of three \bar{q} , while π having only one \bar{q} . The pion recombination function is broad in the momentum fractions x_q and $x_{\bar{q}}$, so with x_q high it is possible for $x_{\bar{q}}$ to be low to reach the region with higher density of \bar{q} . The proton recombination function is much narrower, since the proton mass is nearly at the threshold of the three constituent quark masses. The $x_{\bar{q}}$ values are roughly 1/3 of $x_{\bar{p}}$, so none of the antiquarks can have very low $x_{\bar{q}}$ for $x_{\bar{p}} \sim 0.55$, say. The effect of soft-parton regeneration can therefore drastically increase the \bar{p} production.

It is of interest to point out that the observed \bar{p}/p ratio changes significantly with energy. At $\sqrt{s} = 200$ GeV and $\eta = 3.2$, $R_{\bar{p}/p}$ has been found to be 0.22, which is four times larger than at $\sqrt{s} = 62.4$ GeV [12]. It implies that the degradation effect depends sensitively on \sqrt{s} . It also means that what other ratios have been measured at $\sqrt{s} = 200$ GeV cannot be used reliably as a guide for our present study at 62.4 GeV.

We are now able to relate the average charged multiplicity $(h^+ + h^-)/2$ in the data to $[p + \bar{p} + 1.15(\pi^+ + \pi^-)]/2$ that we can calculate. Since the data on the p_T distribution are taken within the narrow band bounded by $\eta = 3.2 \pm 0.2$, we can determine the x value in the range of p_T of interest by first identifying η with y and use

$$x = \frac{m_T}{\sqrt{s}} e^y, \quad m_T = \left(m_h^2 + \langle p_T \rangle^2 \right)^{1/2}. \quad (27)$$

If we take $\langle p_T \rangle = 1.0$ GeV/c, the corresponding values of x for pion is $x_\pi = 0.4$ and for proton, $x_p = 0.54$, which are well inside the FR.

The slope of the p_T distribution in the semilog plot is essentially determined by the value of T , as prescribed by Eqs. (21) and (22). We find it to be $T = 196$ MeV. In our treatment here and before, the value of T incorporates the effect of radial flow and is therefore larger than the value appropriate for local thermal temperature that is considered in other approaches to recombination [10, 11]. For the values of κ that can reproduce the \bar{p}/p ratio we can calculate $[p + \bar{p} + 1.15(\pi^+ + \pi^-)]/2$, adjusting $\langle p_T \rangle$ in fine-tuning, and obtain the two lines in Fig. 6. The solid line is for $\kappa = 0.76$ and $\langle p_T \rangle = 1.09$ GeV/c, while the dashed line is for $\kappa = 0.72$ and $\langle p_T \rangle = 1.07$ GeV/c. They both fit the data [3] very well. The spectrum being dominated by proton does not depend on κ sensitively; its normalization does depend on the x values, which in turn depend on $\langle p_T \rangle$ for fixed rapidity. For $\langle p_T \rangle \sim 1.08$ GeV/c the corresponding x_p is ~ 0.55 , which is the value we used to calculate \bar{p}/p . Since the contributions from resonance decays have not been considered, our results for $p_T < 1$ GeV/c are not reliable, and should not be taken seriously.

In Fig. 7 we show the p/π ratio for the two cases considered above. Again, there is sensitive dependence on κ , although not as much as in \bar{p}/p . As κ decreases, more soft partons are generated. The increase of \bar{q} enhances π production, and thus suppresses the p/π ratio. The dominance of proton production makes the charged hadron spectrum insensitive to the change in the pion sector. But the ratio manifests the pion yield directly. Currently, the data on the p/π ratio is still unavailable for $\sqrt{s} = 62.4$ GeV. Since κ depends sensitively on \sqrt{s} , the ratio may be quite different from that determined at 200 GeV [14]. To have the ratio exceeding 1 is a definitive signature of recombination at work. The verification of our results will give support to our approach of accounting for hadrons produced up to $p_T = 2.5$ GeV/c at $\eta \simeq 3.2$ in the absence of hard scattering.

We note that the two lines in Fig. 7 are nearly straight, since both p and π distributions are mainly exponential, as shown in Eqs. (21) and (22), except for the prefactor involving p_T for the proton. We therefore expect the measured ratio to be essentially linearly rising in Fig. 7. But more importantly in the first place is whether the ratio exceeds 1 for $p_T > 1$ GeV/c. Our concern should first be whether the regeneration of soft partons and the suppression of hard partons are the major aspects of physics that we have captured in this treatment. The precise p_T dependence of $R_{p/\pi}$, i.e., whether it is linear or not, is of secondary importance at this point. Similarly, we expect the data to show constancy of $R_{\bar{p}/p}$ for the range of p_T studied.

4 Conclusion

We have extended the study of particle production in the FR and TFR to include the regeneration of soft partons due to momentum degradation and to consider also the determination of the p_T distributions. We have shown that the data of BRAHMS for forward production can be reproduced for all p_T , when suitable values for the degradation parameter are obtained by fitting the \bar{p}/p ratio. The consequence is that large p/π ratio must follow. The hadronization process is recombination and the p_T dependence is exponential, reflecting the thermal origin of the partons. We predict that the exponential behavior will continue to higher p_T even beyond the boundary separating FR and TFR. The production of protons is far more efficient than the production of pions. That is not surprising since it is consistent with the result already obtained in [1] due to the scarcity of antiquarks in the FR and TFR. Here, the p_T dependence of the proton-to-pion ratio, $R_{p/\pi}$, is shown to be linearly rising above $p_T = 1$ GeV/c and can become greater than 2 above $p_T = 2.5$ GeV/c. Any model based on fragmentation, whether the transverse momentum is acquired through initial-state interaction or hard scattering, would necessarily lead to the ratio $R_{p/\pi} \ll 1$, by virtue of the nature of the fragmentation functions. In contrast, $R_{\bar{p}/p}$ would be around 1 if gluon fragmentation dominates, and be $\ll 1$ if the fragmentation of valence quarks dominates, so $R_{\bar{p}/p}$ is not the best discriminator between recombination and fragmentation.

No shower partons are involved in the recombination process because hard partons are suppressed in the forward region. That is supported by the absence of power-law behavior in the p_T dependence of the data. Without hard partons there are no jets, yet there are high- p_T particles, which are produced by the recombination of thermal partons only. Thus there can be no jet structure associated with any hadron at any p_T . That is, for a particle (most likely proton) detected at, say, $p_T = 2.5$ GeV/c, and treated as a trigger particle, there should be no associated particles distinguishable from the background. This is a prediction that does not depend on particle identification, and can be checked by appropriate analysis of the data at hand.

Acknowledgment

This work was supported in part, by the U. S. Department of Energy under Grant No. DE-FG02-96ER40972 and by the National Natural Science Foundation of China under Grant No. 10475032.

References

- [1] R. C. Hwa and C. B. Yang, Phys. Rev. C **73**, 044913 (2006).
- [2] B. B. Back *et al.* (PHOBOS Collaboration), Phys. Rev. Lett. **91**, 052303 (2003); Phys. Rev. Lett. **87**, 102303 (2001).
- [3] I. Arsene *et al.* (BRAHMS Collaboration), nucl-ex/0602018.
- [4] K. P. Das and R. C. Hwa, Phys. Lett. **68B**, 459, (1977).
- [5] R. C. Hwa, Phys. Rev. D**22**, 759 (1980); **22**, 1593 (1980).
- [6] R. C. Hwa and C. B. Yang, Phys. Rev. C **66**, 025205 (2002).
- [7] R. C. Hwa and C. B. Yang, Phys. Rev. C **66**, 025204 (2002); Phys. Rev. C **65**, 034905 (2002).
- [8] R. C. Hwa, C. B. Yang and R. J. Fries, Phys. Rev. C **71**, 024902 (2005).
- [9] R. C. Hwa and C. B. Yang, Phys. Rev. C **67**, 034902 (2003); **70**, 024905 (2004).
- [10] V. Greco, C. M. Ko, and P. Lévai, Phys. Rev. Lett. **90**, 202302 (2003); Phys. Rev. C **68**, 034904 (2003).
- [11] R. J. Fries, B. Müller, C. Nonaka and S. A. Bass, Phys. Rev. Lett. **90**, 202303 (2003); Phys. Rev. C **68**, 044902 (2003).
- [12] I. Arsene (for BRAHMS Collaboration), poster contribution at Quark Matter 2006 (to be published in Int. J. Mod. Phys. E).
- [13] H. Yang (for BRAHMS Collaboration), Czech. J. Phys. **56**, A27 (2006).
- [14] M. Murray, Talk given at Hard Probes 06, Asilomar, CA (2006).

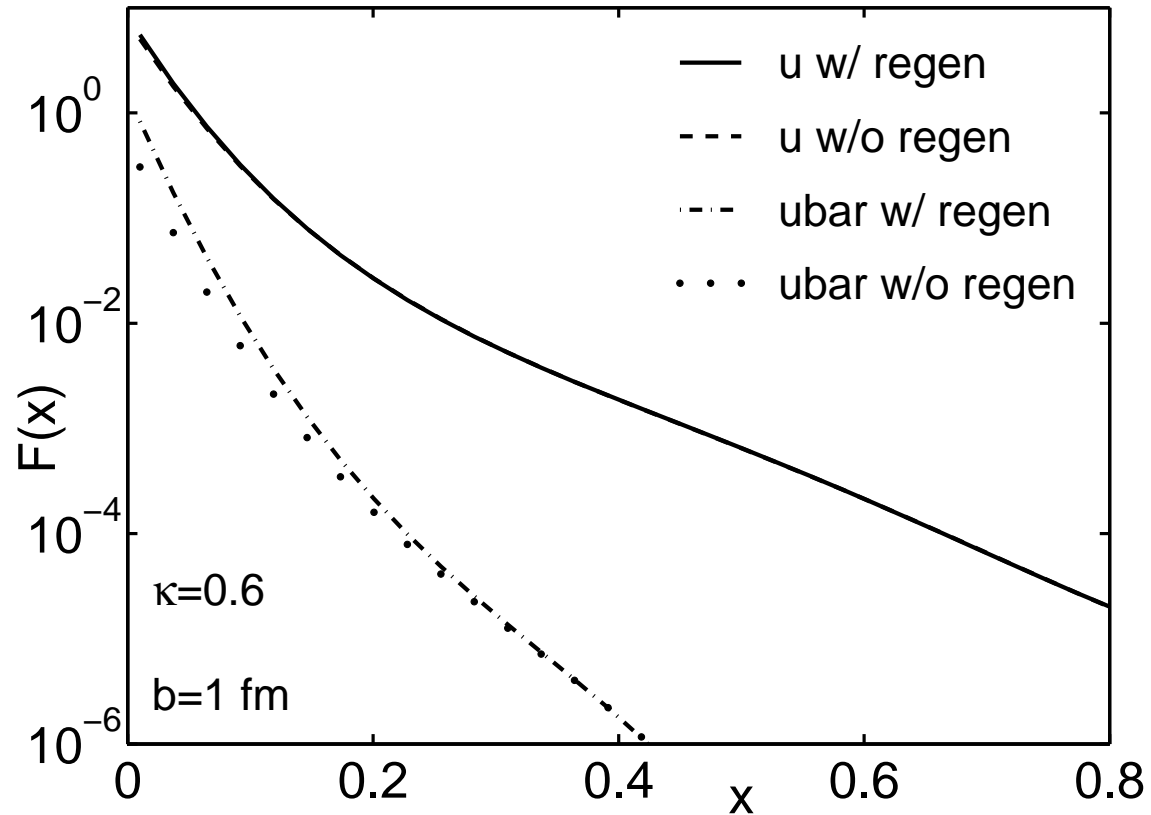


Figure 1: The distributions of u and \bar{u} in momentum fraction x with and without soft-parton regeneration for $\kappa = 0.6$ at $b = 1 \text{ fm}$, where κ is the survival factor in momentum degradation. Solid (dashed-dotted) lines are for u (\bar{u}) with regeneration, while dashed (dotted) lines are for u (\bar{u}) without regeneration.

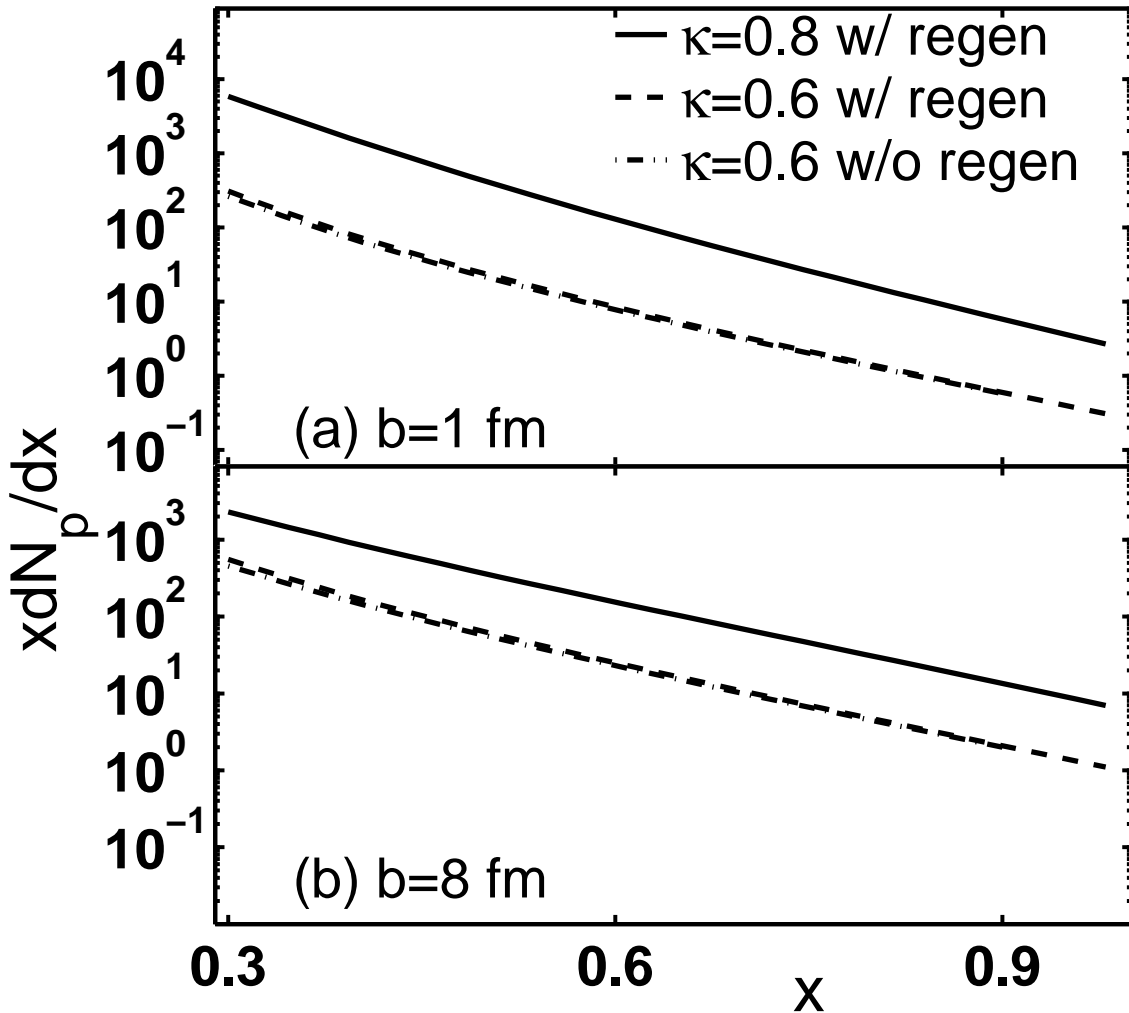


Figure 2: Proton distributions for (a) $b = 1$ fm, and (b) $b = 8$ fm. The solid and dashed lines are for the cases with soft-parton regeneration corresponding to $\kappa = 0.8$ and 0.6 , respectively. The dashed-dotted lines are for $\kappa = 0.6$ without regeneration.

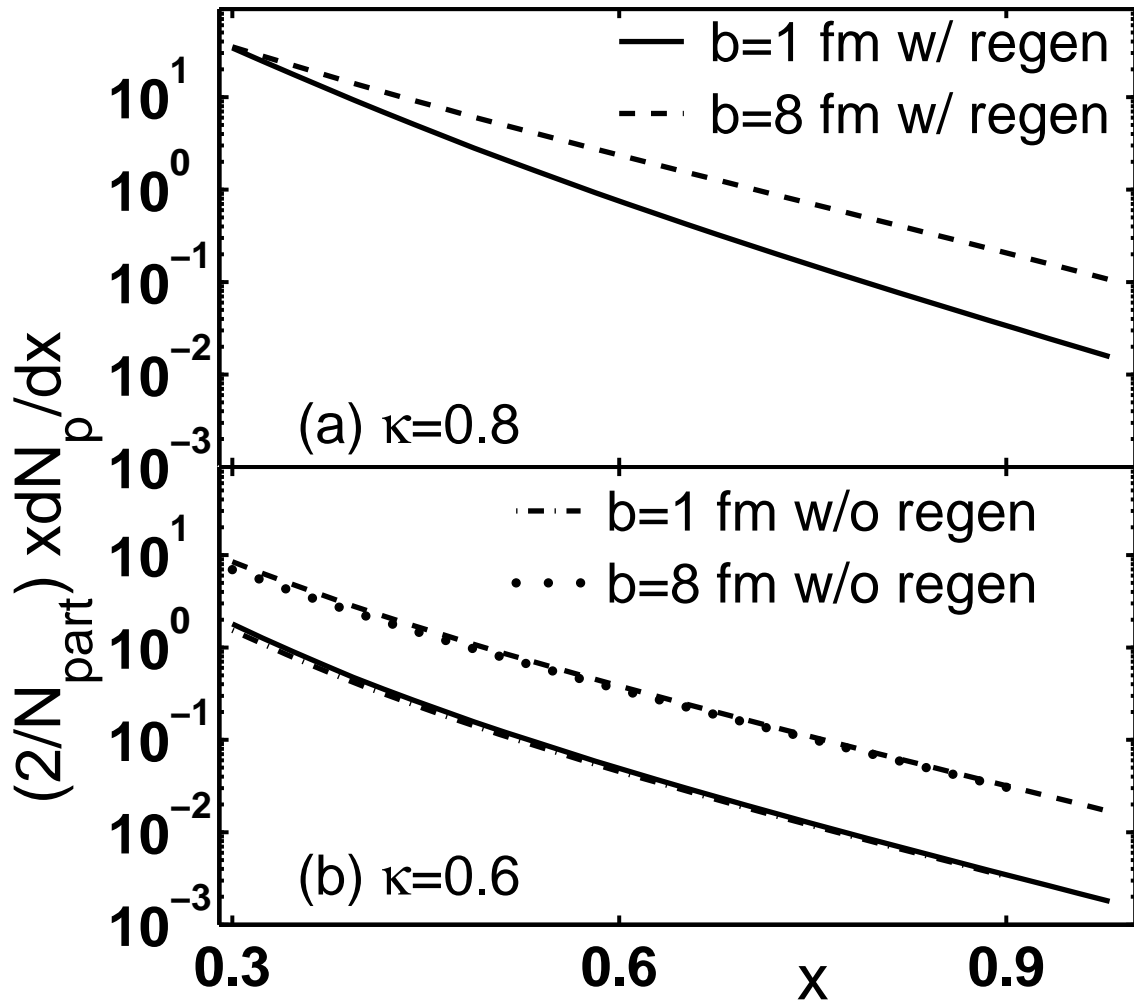


Figure 3: Proton distributions normalized by $N_{\text{part}}/2$ for (a) $\kappa = 0.8$, and (b) $\kappa = 0.6$. The solid (dashed) lines are for the case with regeneration at $b = 1 \text{ fm}$ (8 fm). The dashed-dotted (dotted) lines are for the case without regeneration at $b = 1 \text{ fm}$ (8 fm) and $\kappa = 0.6$.

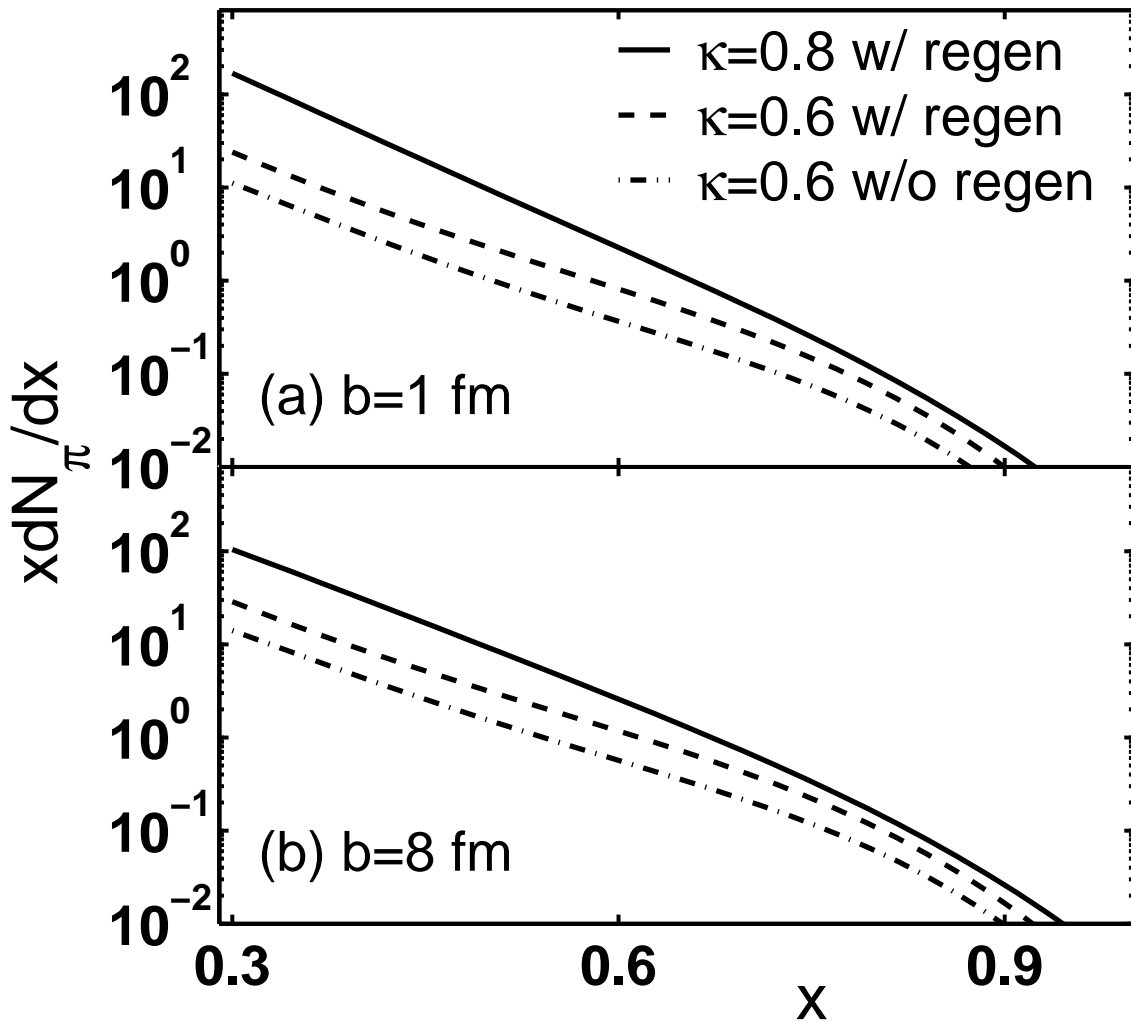


Figure 4: Pion distributions for (a) $b = 1$ fm, and (b) $b = 8$ fm. The lines are as in Fig. 2.

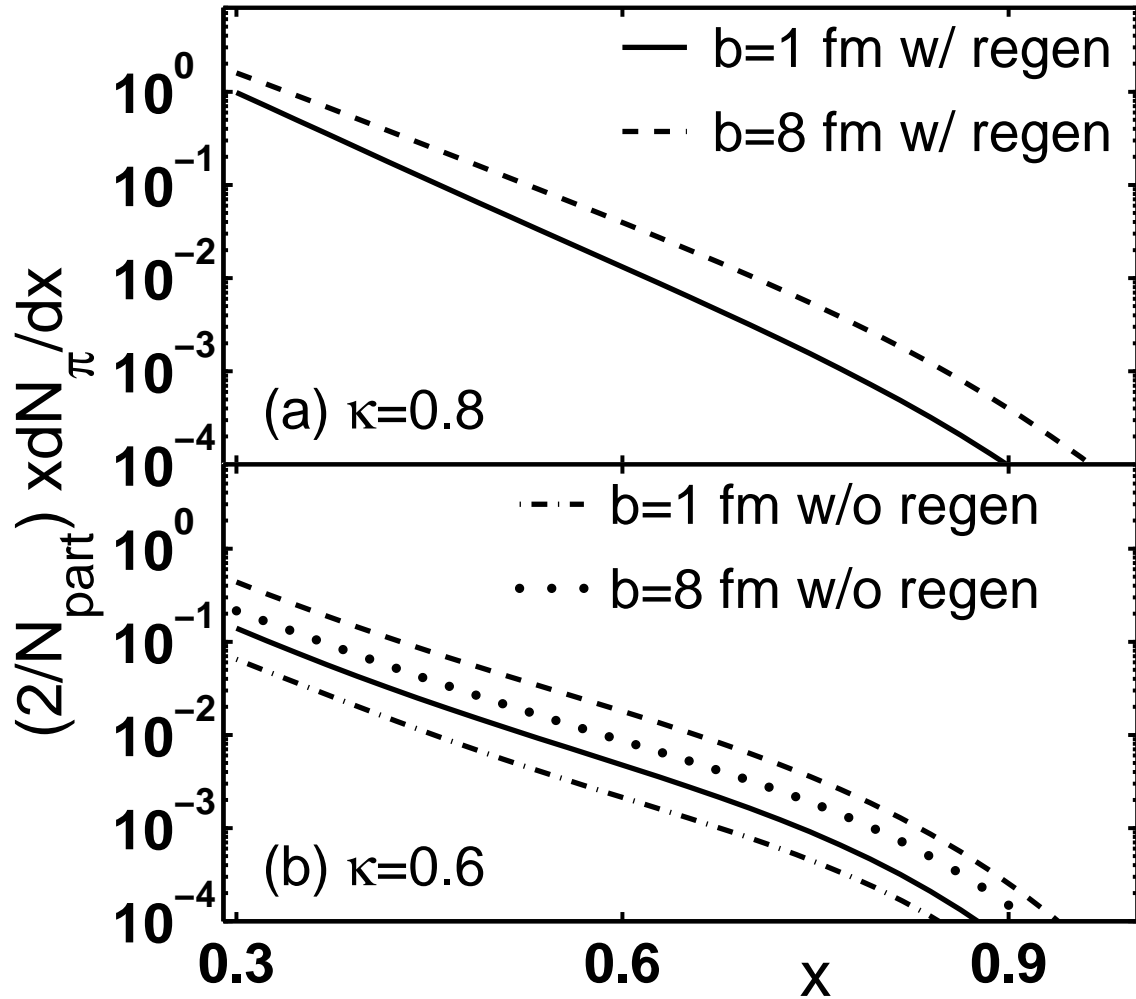


Figure 5: Pion distributions normalized by $N_{\text{part}}/2$ for (a) $\kappa = 0.8$, and (b) $\kappa = 0.6$. The lines are as in Fig. 3.

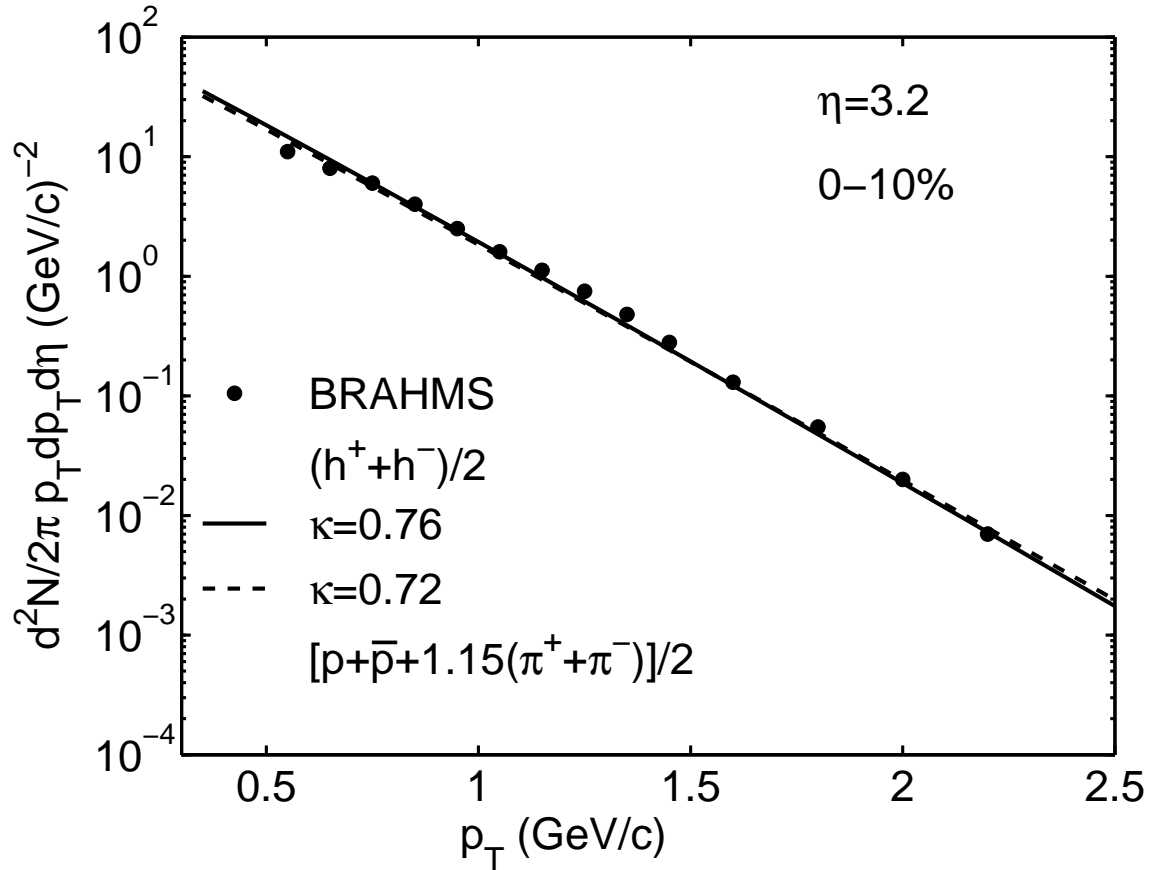


Figure 6: Transverse momentum distribution of charged hadrons produced in Au+Au collisions at $\sqrt{s} = 62.4$ GeV, $\eta = 3.2$ and 0-10% centrality. Data are from [3]. Solid line is for case (a) $\kappa = 0.76$, and dashed line for case (b) $\kappa = 0.72$, calculated in the recombination model for the average charged hadron being approximated by $[p + \bar{p} + 1.15(\pi^+ + \pi^-)]/2$.

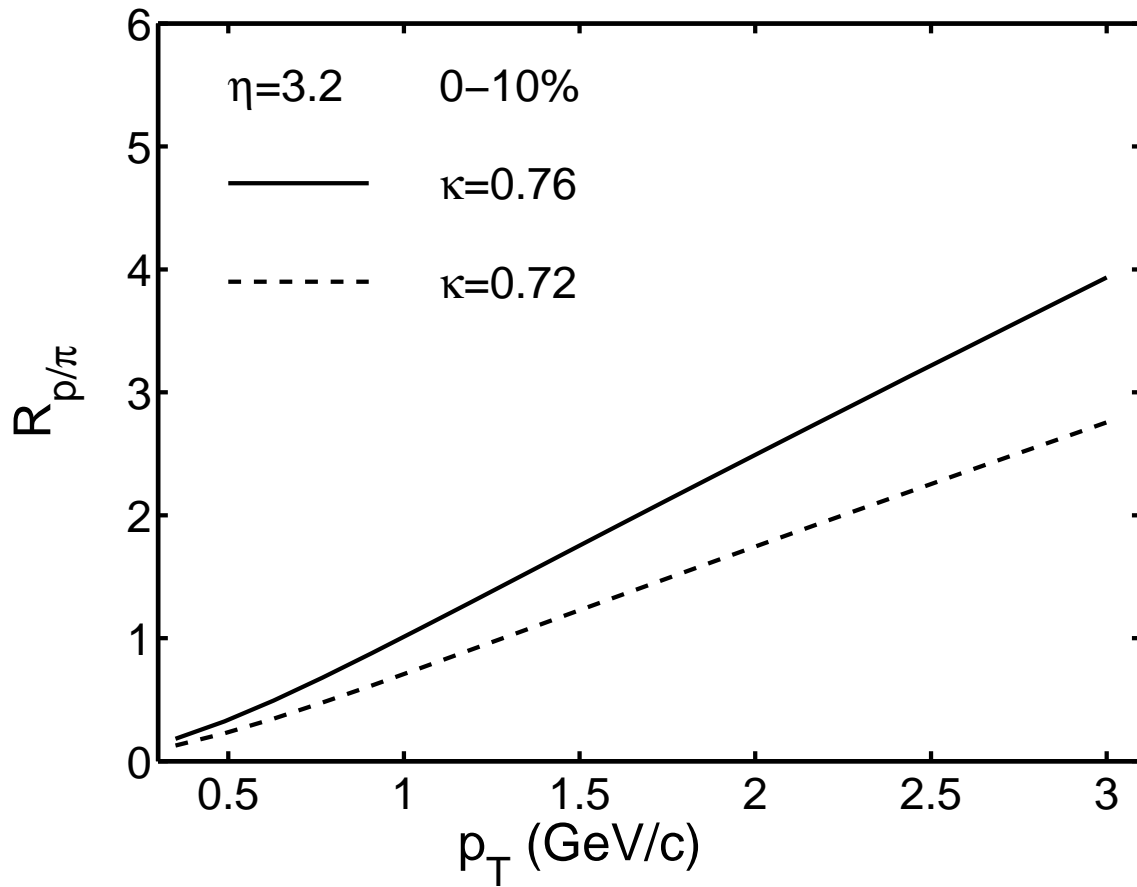


Figure 7: Proton-to-pion ratio calculated for $\kappa = 0.76$ (solid line) and $\kappa = 0.72$ (dashed line) at $\eta = 3.2$ in central Au+Au collisions at $\sqrt{s} = 62.4$ GeV.